Nanoscale

Accepted Manuscript

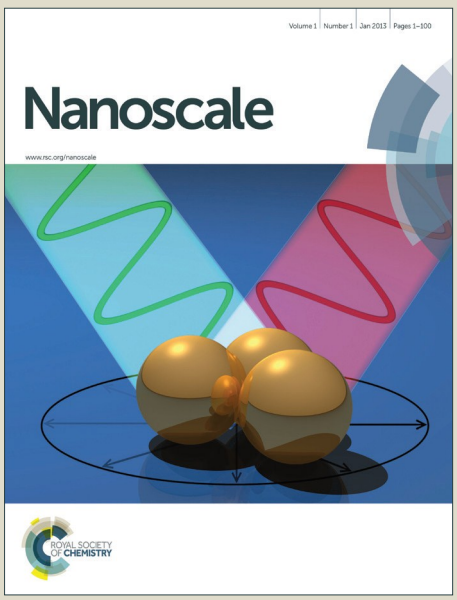

ROYAL SOCIETY OF CHEMISTRY

www.rsc.org/nanoscale

Journal Name

RSCPublishing

ARTICLE

Ru(II)-polypyridyl surface functionalised gold nanoparticles as DNA targeting supramolecular structures and luminescent cellular imaging agents

Miguel Martínez-Calvo,[‡a] Kim N. Orange,[‡b] Robert B. P. Elmes,[a,c] Bjørn la Cour Poulsen,[a] D. Clive Williams*[b] and Thorfinnur Gunnlaugsson*[a]

Cite this: DOI: 10.1039/x0xx00000x

Received
Accepted

DOI: 10.1039/x0xx00000x

www.rsc.org/

The development of 15 nm (average size) Ru(II) functionalized gold nanoparticles **1-3.AuNP** is described. These systems were found to be mono-disperse with a hydrodynamic radius of ca. 1 nm in water but gave rise to the formation of higher order structures in buffered solution. The interaction of **1-3.AuNP** with DNA was also studied by spectroscopic and microscopic methods and suggested the formation of large self-assembly structures in solution. The uptake of **1-3.AuNP** by cancer cells was studied using both confocal fluorescence as well as transmission electron microscopy (TEM), with the aim of investigating their potential as tools for cellular biology. These systems displaying a non-toxic profile with favourable photophysical properties may have application across various biological fields including diagnostics and therapeutics.

Introduction

Nanoparticles (NPs) are defined as solid materials with a nanometric particle size. Metallic nanoparticles, due to their tuneable size, shape and biocompatibility, have been shown to be effective materials for use in biomedical applications, as a vast variety of chemical species can be anchored to their surface.[1] Nanoparticles offer great potential for diagnostic and therapeutic applications over that of single molecules,[2] where intrinsic features such as optical, magnetic, thermal or mechanical properties permit vast potential applications. To date NPs have been capitalised on for use in applications such as in molecular recognition, cellular signalling, drug delivery and sensing/bio-sensing to name just a few key areas.[3] Most recently, the use of NPs to deliver cargo into cells has shown particular promise and has been extensively demonstrated by the work of Mirkin et al.[1a,1d,2k,2l,3a,3d,3k,3o] and Rotello, et al.[1a,1f,2b,2h,3p,3r] The small size of NPs and their large surface area allows anchoring of a large variety of ligands. Gold nanoparticles (AuNPs), in particular are highly attractive inorganic NPs that offer robust frameworks in which several components can be incorporated to give multifunctional capabilities.[2,3] AuNPs are stable structures that can be easily synthesized and functionalized under ambient conditions.[1] AuNPs are thought to be relatively non-cytotoxic as the bulk form of the metal is chemically inert, and any toxicity is usually associated with their surface modified groups/ligands rather than gold itself.[2,3] Mirkin et al., have pioneered the use of AuNPs as drug carriers, photo-responsive therapeutics, imaging agents and gene regulating agents.[3a] Hence, these are clearly highly attractive platforms with great potential for medical applications.

Ruthenium (Ru(II)) based polypyridyl complexes have also been intensively studied to date due to their rich photophysical properties, and they have found application in various fields of research. In particular, Ru(II) based polypyridyl complexes have been developed as sensitive and structure specific luminescent DNA probes and photoreagents.[4] Here, the binding to DNA can occur either through intercalation[5] or by groove binding[6] causing modulation in the photophysical properties of the Ru-complexes; being dictated by the structural and physical nature of the polypyridyl ligands employed. Since targeting DNA with such complexes can prevent DNA replication within cancer cells and induce programmed cell death,[7,8,9] it is of interest to develop new means of delivery into cells. Recently several examples of Ru(II) polypyridyl complexes have exhibited live cellular uptake with many being localized in both nuclei, mitochondria, lysosomes and endoplasmic reticulum.[10] However, to date, examples of Ru(II) functionalised NPs, which provide possibility of delivering high concentrations of Ru(II) complexes into live cells, remain few.[11] Pikramenou and co workers have recently studied the luminescent properties of several Ru(II) functionalised NPs,[11j,k] coated with a fluorinated surfactant, and shown that the emission properties (including lifetimes and quantum yields) of such conjugated systems is (AuNP) distance depended and can

be enhanced over the individual complexes, which is highly desirable for application in biology. We have recently developed cell targeted probes capable of penetrating cells and inducing apoptosis using both organic, as well as metal ion complexes.[12,13] In addition to these studies our group was the first to demonstrate the use of luminescent Ru(II)-polypyridyl conjugated to AuNP (Ru(II)-AuNPs). While we demonstrated that the photophysical properties of the Ru(II) complexes were preserved, the small size of AuNPs used, (average size of 4-5 nm), limited their applications, where it proved difficult to further investigate and characterize their uptake mechanism in cancer cells.[11a] As the size of the **AuNP** is know to be able to strongly influence the chemistry and the physical properties of the surfaced functionalised ligands themselves (e.g. due to backing, self-assembly interactions, *etc*.), as well as the their biological properties (interactions with membrane bound proteins, *etc*.), we set out to investigate the use of larger AuNPs for cellular applications, in the hope of profiling the mechanism of cellular uptake in more detail and their subsequent distribution in the cytosol of such Ru(II)-AuNPs conjugates. We foresaw that our investigations would contribute to the general understanding of the behaviour of such nano-structures in biological environment to their possible application in biological media; particular in imaging and for the delivery of novel targeting therapeutics. To enable a direct comparison with our previous work, we have synthesized the polypyridyl complexes **1**, **2** and **3**, which have been tethered, *via* a phen spacer, to AuNPs with a larger diameter of *ca.* 30-40 nm (**1.AuNP**, **2.AuNP** and **3.AuNP**, Figure 1). Herein, we present our results, where we undertaken a detailed investigation of the physical and photophysical properties of these new nanostructures, their ability to interact with DNA and their biological activities in a cervical cancer cell line, using confocal fluorescence and transmission electron microscopy', which demonstrates that while the increasing size of the AuNP allows for cellular uptakes studies to be profiled more accurately, the enhanced populate of the complexes at the AuNP surface greatly affects their application due to increased inter- and intramolecular interactions.

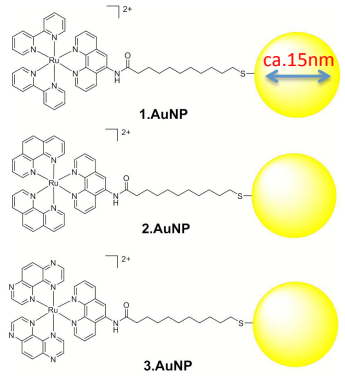

Figure 1. The Ru(II)polypyridyl complexes-AuNP hybrid materials **1-3.AuNP** on 15 nm gold nanoparticles developed for this study. These were formed by surface modification of freshly made AuNP using the thiol-terminal conjugated complexes **1-3** (See ESI for detail).

Results and Discussion

Synthesis and characterisation of 1-3.AuNP

The synthesis of **1-3** was achieved according to Scheme S1 (see ESI). This involved the formation of the Ru(II) precursors cis-[$Ru(bpy)_2Cl_2$], cis-[$Ru(TAP)_2Cl_2$], [$RuCl_2(\eta^4$-COD)] in accordance with established literature procedures, which were then reacted with phen derivative **4** (See ESI, Scheme 1) 11-mercapto-*N*-(1,10-phenanthrolin-5-yl)-undecanamide in a single step using a peptide coupling reaction.[11a] All the complexes were analysed using conventional methods (See ESI), the absorption spectra of each in water and buffered pH 7.4 solution are included in the ESI. The AuNP employed, in the formation of **1-3.AuNP**, were formed using the established sodium citrate method, which resulted in the formation of ca. 15-20 nm AuNP according to TEM analysis.[14]

The formation of **1-3.AuNP** was achieved by carrying out surface modification of the AuNPs in water (See Experimental). In the case of **1-3.AuNP**, this involved the addition of the appropriate Ru complex (in water) to an aqueous solution of AuNPs. Adjustment of the pH of the reaction to pH 3, using HCl, followed by stirring at room temperature for 12 hours provided the desired Ru(II) functionalized AuNPs **1-3.AuNP**. Purification was achieved by addition of a concentrated solution of ammonium hexafluorophosphate to an aqueous solution of **1-3.AuNP**, followed by centrifugation, where the isolated solid was washed with MeOH. A second anion exchange process was achieved by firstly dissolving the isolated solid in CH_3CN, before addition of a concentrated solution of tetrabutylammonium chloride. The resulting suspension was then centrifuged, and the isolated dark solid was washed with acetone. The full upload over the surface of the AuNP will compromise *ca.* 3000-4000 of the Ru(II) complexes **1-3**.[13e] The resulting surface modified AuNPs were analysed using UV-Vis absorption spectroscopy, Dynamic Light Scattering (DLS) and Transmission Electron Microscopy (TEM) imaging in both water and in buffered solution at pH 7.4. Recording the Zeta potential, gave rise to a positive potential of 19 mV in the case of **3.AuNP**, indicating the cationic nature of the AuNP after surface modification with **3**. In the cases of **1-2.AuNP** the value obtained for the Zeta potential was closer to be 0 mV, indicating that these conjugates were not colloidally stable. Nevertheless, we decided to study the photophysical properties and the uptake mechanism of these conjugates for comparative reasons with our previous 4-5 nm Ru-AuNP conjugates.[13a]

The UV-Visible absorption spectra of bare AuNPs and **1-3.AuNP** are shown in Figure 2, measured in water (Figure 2a), and in 10 mM phosphate buffer at pH 7.4, Figure 2b. In both solutions, the bare AuNP SPR band was centred at 524 nm, demonstrating that it was not dependent on the media. In contrast, the surface modification of AuNP by complexes **1-3** gave rise to a red shift in the absorption spectra of the SPR

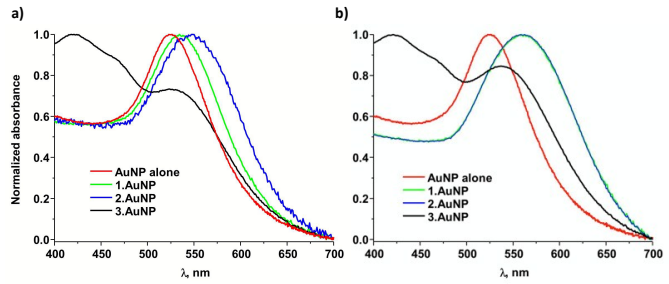

Figure 2. The UV-Visible absorption spectra of **1**-**3.AuNP** in: (a) water and (b) in pH 7.4 phosphate buffered solutions.

band (shown as normalized spectra in Figure 2) for all three complexes, in both media. In both solvent media the MLCT band of the Ru(II) polypyridyl complexes was also visible for **3.AuNP**; the MLCT bands of **1.AuNP** and **2.AuNP** were masked by the SPR band of the AuNP itself. However, the higher energy Ru(II) polypyridyl band is clearly visible (See ESI, and later discussion). In the case of **3.AuNP** the MLCT transitions can be seen as broad bands, centred at 417 nm with a shoulder at 455 nm, structurally matching that of complex **3** itself (c.f. the UV-Vis spectra of **1-3** in the ESI). As can be seen from Figure 2a, when recorded in water, the SPR band was centred for **1-3.AuNP** at 535 nm, 547 nm and 525 nm for these modified AuNPs, respectively. These solutions were found to be stable over a period of several months, as only very minor changes were observed in the UV-Vis absorption spectra. The stability in solution of **3.AuNP** was further monitored by recording the UV-Vis absorption spectra over 16 hours.

Whilst over the first 6 hours no changes were observed, a small reduction (5%) in absorbance was seen between 6-10 hours for the SPR band. In contrast to that seen in water, in pH 7.4 phosphate buffered solution, Figure 2b, the absorption spectra of **1-3.AuNP** were slightly red shifted. Here, both **1.AuNP** and **2.AuNP** appeared identical, being centred at 560 nm, whilst the SPR band for **3.AuNP** was centred at 535 nm. Such a shift of ca. 15-20 nm is an indication of an agglomeration effect in the case of **1.AuNP** and **2.AuNP**. In the case of **3.AuNP**, stability measurements were also carried out, by observing the changes in the absorption spectra over 16 hours. Unlike that seen in water, no changes (within experimental error) were seen in the SPR band of **3.AuNP** over this time period, indicating that **3.AuNP** was less susceptible to aggregation in pH 7.4 buffered solutions. We also carried out stability measurements in the presence of 160 mM NaCl, which again did not give rise to changes in the absorption spectra of **3.AuNP** over period of 16 hours.

The luminescent properties of these surfaced modified AuNPs were also investigated. The excitation of **1-3.AuNPs** (at the λ_{max} for all the MLCT bands as determined for **1-3**) gave rise to MLCT centered emission at long wavelengths (see discussion below) typical of that seen for such complexes. Moreover, the excitation spectra of these AuNPs also gave rise to spectra that were structurally similar to those observed for the absorption spectra of the complexes alone (See ESI). However, as

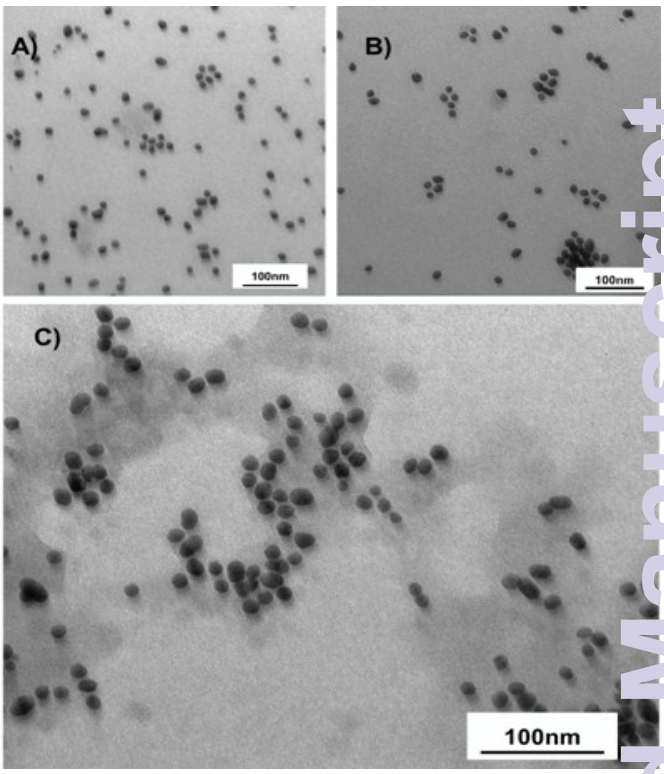

Figure 3. TEM images obtained using functionalized nanoparticles: (a) **1.AuN** (b) **2.AuNP**, (c) **3.AuNP**.

previously observed, **1-3.AuNP** displayed reduced emission in comparison to their parent complexes **1-3**, despite the fact that the complexes are separated from the gold by a covalent spacer.[15]

To investigate the structural nature of these surface modified AuNPs further, both TEM and DLS analysis were carried out. The DLS analysis (See ESI) of these AuNPs in deionized water revealed that the hydrodynamic radii of **1.AuNP** and **3.AuNP** were in the expected region of ca. 15 nm, while **2.AuNP** gave rise to larger structures in solution, being ca. twice of that obtained for **1.AuNP** and **3.AuNP**. However when these measurements were repeated in 10 mM phosphate buffer at pH 7.4 the hydrodynamic radius increased for **1-3.AuNP** compared to that seen in deionized water (See ESI) indicating some degree of agglomeration. Of these, the hydrodynamic radius of **3.AuNP** increased the least, with an ionic radius of ca. 15 nm, while both **1.AuNP** and **2.AuNP** showed the formation of much larger structures with hydrodynamic radii of ca. 100 nm in solution. These results indicate that **1-3.AuNP** are susceptible to some degree of aggregation in buffered solution. TEM images obtained for **1-3.AuNP** in water are shown in Figure 3, and clearly show monodisperse spherical nanoparticles. The measured average sizes of the core of the AuNPs were determined as 15.3 ± 3.0, 15.4 ± 3.3 and 15.8 ± 3.8 nm for **1.AuNP**, **2.AuNP** and **3.AuNP** respectively.

In contrast, the TEM imaging of **1-3.AuNP** in 10 mM phosphate buffer solutions are shown in Figure 4 and confirm the formation of agglomerates of **1.AuNP** and **2.AuNP**, where aggregation of **2.AuNP** was particularly apparent. In contrast

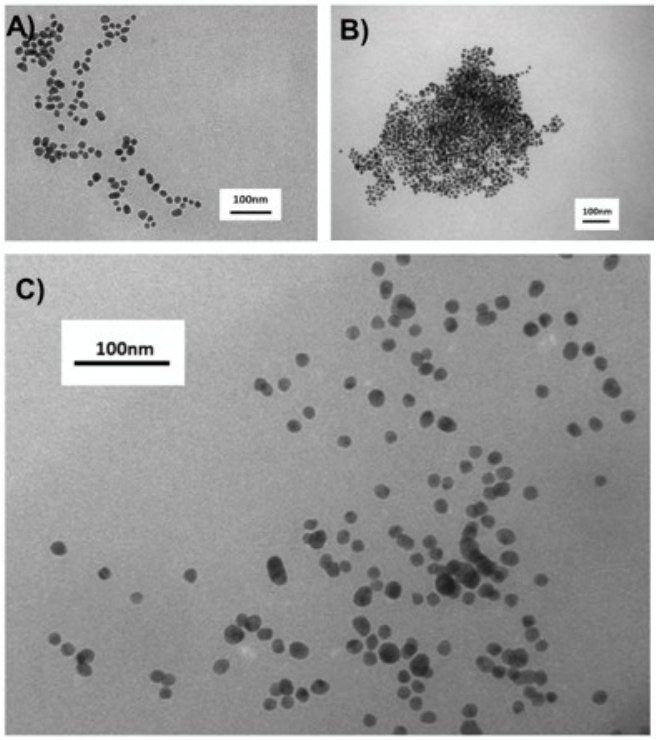

Figure 4. TEM images obtained using functionalized nanoparticles: (a) **1.AuNP**, (b) **2.AuNP**, (c) **3.AuNP** in 10 mM phosphate buffer.

3.AuNP did not give rise to any obvious aggregate formation, supporting the results observed through DLS analysis. Such behavior may be due to the known ability of the TAP ligand and related Ru(II) TAP based complexes to participate in hydrogen bonding with protic solvents thereby reducing their tendency to aggregate. In fact, the hydrogen bonding capability of the TAP ligands has been shown to play an important role in their interaction with the DNA and this may be an important factor when considering their potential in biological applications.[16] To further investigate these effects we proceeded to study the binding behaviour of all three systems with double stranded DNA in solution.

Photophysical Analysis of 1.AuNP-3.AuNP with *st*-DNA

Having carried out the above photophysical evaluations of **1-3.AuNP** in water and buffered solutions, we conducted photophysical studies to establish the interaction of these compounds with double stranded DNA. This was achieved using UV-vis absorption, fluorescence emission and circular dichroism spectroscopy, in 10 mM phosphate buffered solution at pH 7.4 in the presence of salmon testes (st) DNA. The changes upon binding of complexes **1-3** to DNA has previously been investigated in our laboratory and showed that all three complexes to have high affinity for st-DNA, with binding constants of 5.5-6.5 x 10^5 M^{-1} in this phosphate buffer at pH 7.4.[11a] All measurements were repeated in triplicate using various batches of **1-3.AuNP** to ensure reproducibility.

The changes observed in the absorbance spectrum of **3.AuNP** upon titration of these AuNPs with st-DNA, are shown in

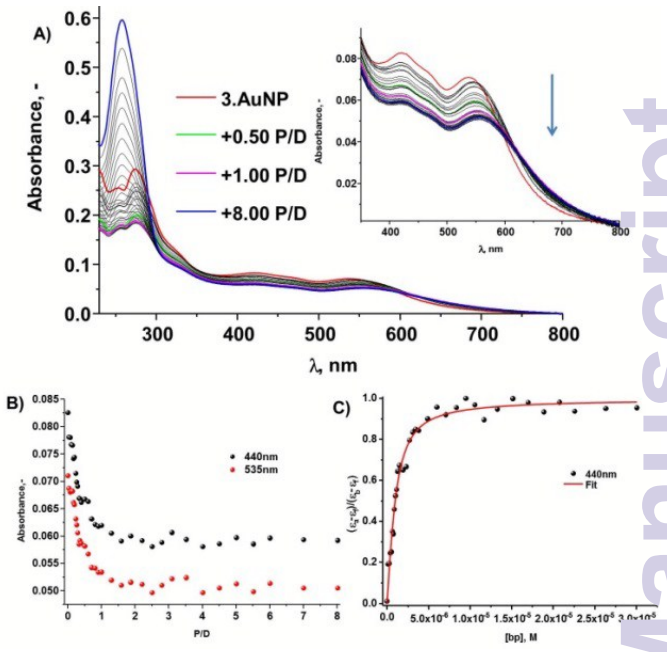

Figure 5. (A) Representation of the UV-Vis titration of **3.AuNP** with st-DNA (inset zoom of the region from 350 to 800 nm); (B) binding isotherms of the MLCT band at 440nm and the SPR band 535 nm and (C) Bard fitting plot of the MLCT band cantered at 440 nm.

Figure 5a. Each absorption band was clearly affected upon addition of aliquots of DNA; 282 nm (due to the transitions of the ancillary ligands, π-π*; ε = 50900 M^{-1} cm^{-1}), MLCT band centred at 418 nm (ε = 10700 M^{-1} cm^{-1}) a shoulder at 462 nm and in the SPR band at 535 nm. Abrupt changes were observed in the higher energy transitions, as well as in the MLCT band which underwent a 29% hypochromic displacement, with a similar (26%) effect being observed for the SPR band centred at 535 nm within the addition of 0→1 P/D (Phosphate/Dye ratio), with further changes occurring up to the addition of 2.5 P/D, as demonstrated in Figure 5b. These are similar changes to those observed for the complex alone upon titration with st-DNA;[11a] which are consistent with strong association of **3.AuNP** with DNA. The intrinsic binding constant K_b, was also determined using the model of Bard et al. using these changes.[17] A representative plot of $(\varepsilon_a - \varepsilon_f)/(\varepsilon_b - \varepsilon_f)$ vs. [base pairs] and the corresponding best fit of the data to the Bard equation (R = 0.98) is shown if Figure 5c. From these changes, a binding constant K_b of 2.4 x 10^6 M^{-1} was determined. This is a comparable binding affinity to that seen for other Ru(II) complexes, under such experimental conditions.[18] The value obtained for the binding site for these titrations is unity and an indication that **3.AuNP** interacts with the DNA by groove binding, or electrostatic binding, since this value is much lower than the expected value of two commonly seen for interaction by intercalation.[17] This is not surprising giving that the conjugation of these complexes to the AuNPs will have an effect on the degree of freedom for the binding of these to the biomolecule.

The high affinity of **3.AuNP** and the strong interaction observed in the absorption spectra was further confirmed by

observing the changes in the fluorescence emission spectra upon excitation at 440 nm. The overall changes in MLCT emission (centred at 637 nm) are shown in Figure 6, demonstrating that the MLCT emission was quenched by ca. 70%, after the addition of 0.5 P/D of st DNA (as shown as inset in Figure 6); being blue-shifted by ca. 15 nm. Once more, spectroscopic changes of this nature are in agreement with results obtained previously by our group[11a] and by others for similar Ru(II)-polypyridyl complexes containing two TAP ligands which have been shown to photo-oxidise *guanine* containing nucleotides through a proton coupled photoinduced electron transfer (PCET) process.[19]

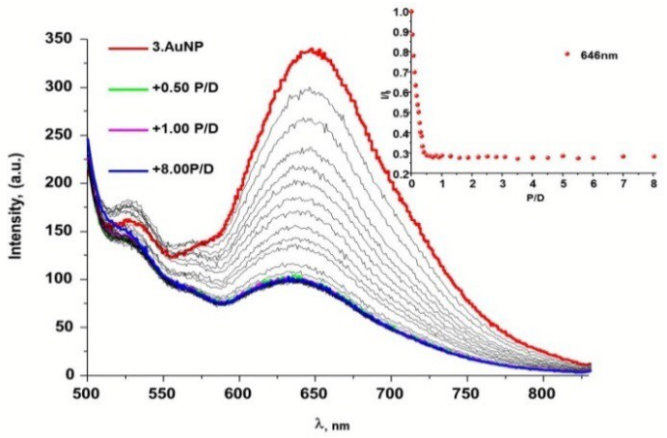

Figure 6. Emission spectra of **3.AuNP** during its titration with st-DNA (inset, the binding isotherm at 646 nm).

For comparison with our previously reported Ru-AuNPs, we also carried out the titration of **1-2.AuNP** with st-DNA. Prior to the titration, the absorbance spectrum of **1.AuNP** (c.f. ESI, and discussion above) possess two bands, one centred at 262 nm (ε = 49500 M^{-1} cm^{-1}) corresponding to the π-π* transitions of the ancillary ligands of the Ru(II) which were monitored upon titration with DNA as the MLCT band was masked by the SPR band of the AuNP. These transitions were blue shifted by ca. 10 nm compared to the free complex (possibly due to the π-π stacking interactions between the aromatic rings of neighbouring molecules of **1**).[20] Upon increasing addition of st-DNA the π-π* transition initially underwent a hypochromic shift up to 1-1.5 P/D followed by a hyperchromic shift thereafter. A slight red hypochromic shift was also observed in the SPR band upon addition of DNA up to 2 P/D (Figure S9A). A very similar effect was observed in the absorption spectrum of **2.AuNP** upon carrying out such DNA titrations (monitoring both the 266 nm ε = 72700 M^{-1} cm^{-1} and the MLCT transitions, see ESI). Excitation of **1-2.AuNP** at 420 nm, corresponding to the MLCT band, gave rise to an MLCT emission centred at 600 nm, which was structurally similar to that of the free complex (excitation spectra confirmed this as well). However, upon addition of st-DNA, no significant changes were observed in the MLCT centred emission spectra. These results confirmed that the agglomeration of **1-2.AuNP** showed by the TEM imaging is hindering these conjugates to interact with the st-DNA. In our previous study with 4-5nm **Ru-AuNP** conjugates all of them were able to interact with the stDNA whereas in our new conjugates it was possible to study in detail the **3.AuNP** derivative. This could be due to the different stabilization of the AuNP. In our previous work the surfactant TOAB was employed to prevent aggregation of the AuNP. However, in the present work sodium citrate was employed, making that the coating of the gold surface implicated the removal of the citrate and the consequent aggregation of the **Ru-AuNP** with the exception of **3.AuNP** where the availability of the TAP ligands to form H-Bonds prevents their aggregation and allows their interaction with the stDNA in a similar manner than the previous 4-5 **Ru-AuNP**.

To further study the interaction of these modified AuNP conjugates with DNA, CD-titrations were also carried out (See ESI), by adding various concentrations of **1-3.AuNP** to a solution of st-DNA and monitoring the changes in the DNA CD spectra between 200-300 nm. Significant induced changes were observed for the CD-spectra in the presence of **1-3.AuNP**. The DNA transitions,[21] seen as a positive CD-band at 280 nm and a negative CD-band at 250 nm were affected, but no long wavelength transitions were observed. For **1-3.AuNP**, the long wavelength DNA-transition was reduced in intensity, while lesser changes were seen in the higher energy CD-band. Of these, the order of changes were largest in the case of **2.AuNP** and **3.AuNP**, where the 280 nm band was almost fully reduced to zero, in the case of **3.AuNP**, or with a slight cross over to a negative signal in the case of **2.AuNP**. While these titrations did not induce changes in the MLCT band the loss of the right handed helical structure in these CD measurements serve to confirm the above results where it is clear that **1-3.AuNPs** are causing some changes to the double helical structure.

Thermal Denaturation and Cleavage Ability of 1-3.AuNP with *st*-DNA and plasmid DNA, respectively

Having investigated the interactions of **1-3.AuNP** with double stranded DNA using various titration experiments, thermal denaturation studies were also carried out on st-DNA in the presence of **1-3.AuNP** ; In the absence of these nano-structures a T_m value of 69.8 ºC was determined for the st-DNA under the experimental conditions used. Complexes **1-3** were all shown to stabilize double stranded DNA prior to their conjugation to the AuNPs (See ESI). The melting profiles of st-DNA upon interaction with **1-3.AuNP** (See ESI) were measured at P/D = 10, and all showed only minor changes in the T_m values; these being most pronounced with **2.AuNP** and **3.AuNP**, both of which showed a slight increase in the T_m (70.2 ºC). These results are similar to that seen for smaller AuNPs previously developed in our laboratory[11a] and indicate that the conjugation of Ru(II) complexes to the AuNP surface seems to alter their ability to stabilize double stranded DNA.

The DNA photocleavage efficiencies of **1-3.AuNP** were also compared to the known DNA photocleavage agent $[Ru(bpy)_3]^{2+}$ by treating pBR322 plasmid DNA (1 mg mL^{-1}) (See Figure and Table S1 in ESI) with each of the Ru(II) AuNPs.[22] As above, the complexes **1-3**, all gave rise to nicking of plasmid DNA,

determined using horizontal agarose gel electrophoresis. However, **3.AuNP** showed lower cleavage ability compared to the free complex **3**, with a 2.1%, 4.6% and 5.4% conversion to open form DNA at P/D ratios of 20, 10 and 5, respectively; and this small capability was removed in the presence of NaN_3. It is clear that whilst the above spectroscopic titration results, clearly demonstrate high affinity of **3.AuNP** for DNA, the thermal denaturation measurements do not seem to lead to increased stability in double stranded DNA. Moreover, it is clear that **3.AuNP** does cleave DNA to some small extent in the presence of light activation, as had been seen for **3**. These results clearly demonstrate that surface modification of AuNP with **3**, has a major effect on the ability of the Ru(II) complex to either stabilize or cleave DNA; commonly seen properties for Ru(II)-polypyridine complexes. Hence, the results above suggest that these systems would not function as therapeutic candidates, but their potential as luminescent biological imaging agents or as carriers for other drug substrates (or other type of cargo, such as in gene-delivery, c.f. discussion in introduction section) is feasible. Therefore the potential as luminescent biological imaging agents was investigated further and will be discussed below. However, the cause for the lack of these nano-structures to carry out functions (i.e. stabiles or cleave DNA) seen for the complexes **1-3** alone, seem to stem from their functionalisation to AuNP. Above TEM and DLS results strongly suggested media dependent agglomeration of **1.AuNP** and **2.AuNP** with the effect being less pronounced for **3.AuNP**. In order to investigate these results further, we explored the binding of these nanostructures to st-DNA using both DLS and TEM analysis.

DLS and TEM studies of 1-3.AuNP with DNA

The DLS studies of **1-3.AuNP** with st-DNA were carried out in 10 mM phosphate buffered solution at different P/D ratios. These studies (See Figure 7 and ESI) confirmed the results of the spectroscopic studies above, where upon interaction with DNA, binding or some sort of self-assembly formation occurred which led to significant agglomeration in the case of **1.AuNP** and **2.AuNP**, with an increase in the hydrodynamic radius of these systems. Given that Ru(II)-polypyridyl complexes are well known to either groove bind or intercalate with DNA, it is not unreasonable to expect that such a phenomenon might be occurring. In the case of **3.AuNP**, these particles have a diameter in solution of about 36 nm that increased regularly with the addition of st-DNA up to 0.23 P/D. Such behaviour clearly demonstrates a gradual self-assembly formation between these particles and DNA, where the self-assembly reached an average diameter of 500 nm. Subsequent additions of st-DNA, from 1→100 P/D, did not produce any further changes in the measured diameter of these DNA aggregated particles. This was further demonstrated by TEM analysis as observed in Figure 8 showing the TEM images of **3.AuNP** in the presence of DNA. In the case of conjugates **1.AuNP** and **2.AuNP** (Figures S16-S17) there was a similar pattern for values of P/D (~0.20), however, at higher values of P/D the particle diameter varied randomly, which could

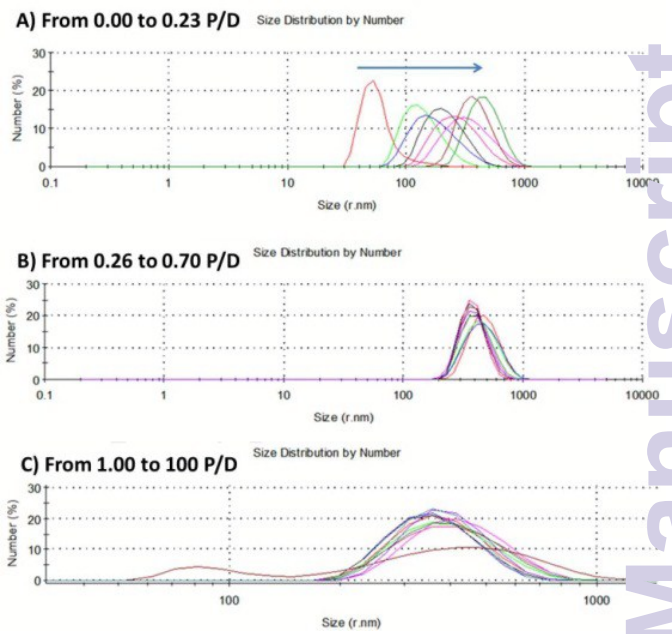

Figure 7. Changes in the DLS in 10 mM buffered solution of the size distribution of **3.AuNPs** upon increasing concentration of st-DNA (expressed as P/D values): (a) The gradual changes occurring between 0 (shown in red) to 0.23 P/D (... right green curve). (b) The changes between 0.23→0.70 P/D. (c) zoomed in on ... the larger DNA agglomerated **3.AuNPs** changes occurring from 1.00→100 P/D. These measurements were repeated three times using freshly made solutions.

indicate a weaker interaction than in the case of **3.AuNP**. T... confirm these results further, TEM studies were carried out using samples of **1-3.AuNP** treated with different ratios of s... DNA (P/D of 0, 0.23, 1.00 and 8.00, respectively) in 10 mM phosphate buffer solutions. The results for 3.AuNP are show... in Figure 8 (See ESI for **1.AuNP** and **2.AuNP**). Comparing Figure 8a with that of Figure 8b, it is clear that initially th... nanoparticles are more monodisperse while at a P/D-ratio =

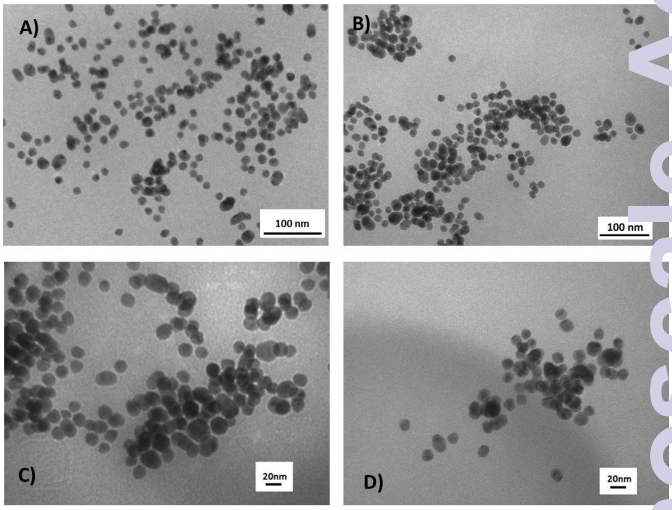

Figure 8. Images obtained of **3.AuNP** by TEM at different P/D ratios: (a) in absence of any DNA; (b) P/D = 0.23, (c) P/D = 1.00, (d) P/D = 8.00.

0.23, clusters are beginning to form due to interaction with the st-DNA. Upon further increasing the P/D ratio, the self-assembly formation between **3.AuNP** and st-DNA, is even more apparent as seen in Figures 8c and 8d, respectively.

In the case of **1.AuNP** continuous increments of the size of the AuNPs aggregates were observed with the addition of the increasing concentrations of st-DNA (c.f. ESI). While in the case of **2.AuNP** fast agglomeration of these nanoparticles (c.f. ESI) occurred instantly upon addition of st-DNA. These TEM results confirm a strong self-assembly interaction with st-DNA

investigated both with and without light irradiation; the latter being carried out in order to establish, if these systems were phototoxic, particularly in the case of **3.AuNP**, which is known to form adducts with DNA upon irradiation. The HeLa cells were initially treated in the dark and either remained incubated in the dark or exposed to mild irradiation of 4 J/m² of light. Hela cells treated with **3.AuNP** and incubated in the dark did not show a reduction in cell viability when compared to the untreated control cells, indicating that these AuNPs were not cytotoxic in the dark. Upon light irradiation there was a small

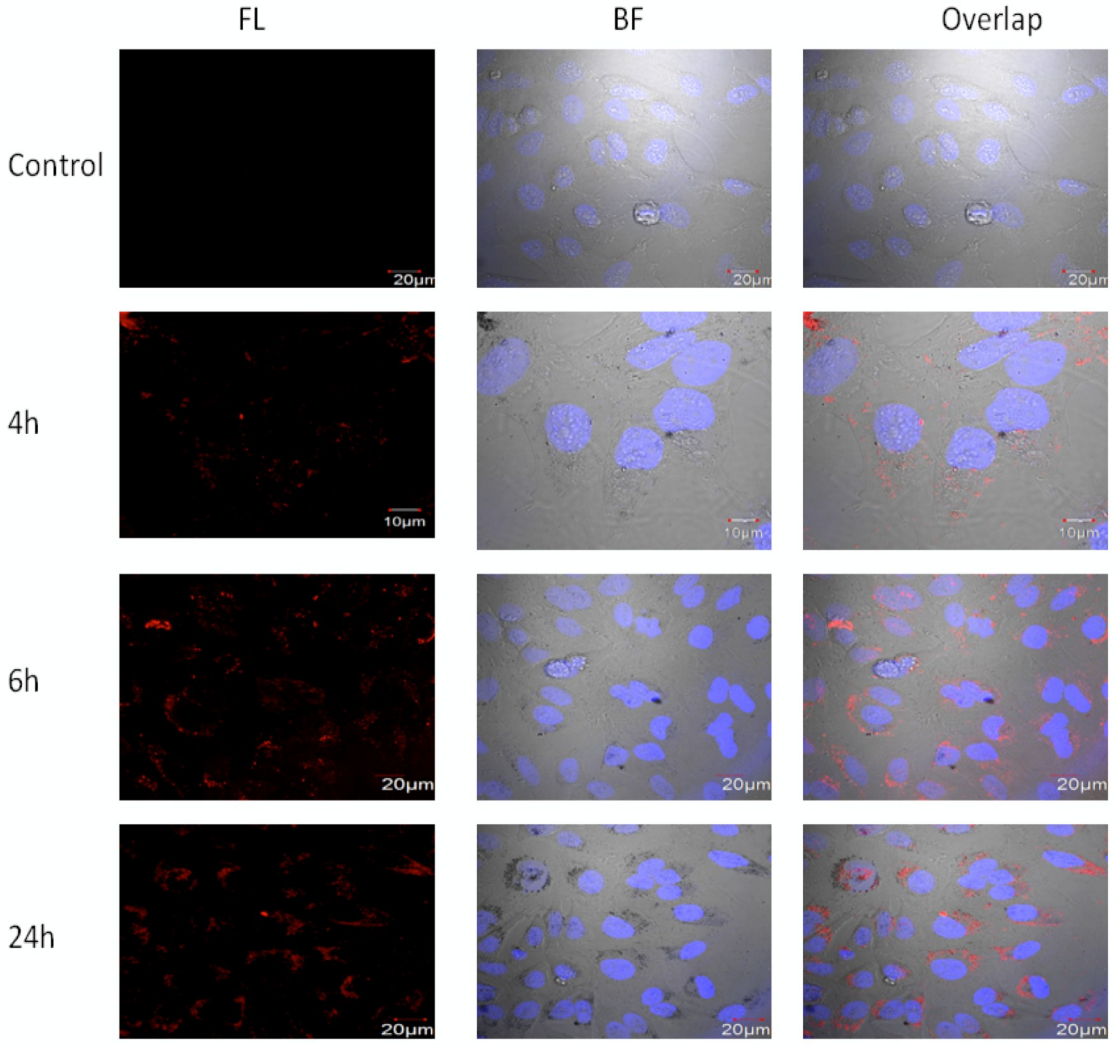

Figure 10. Confocal fluorescence microscopy images of HeLa cells treated with **3.AuNP** for 2-24 h. Fluorescence images (FL) where nuclear stain DAPI is blue and **3.AuNP** in red and bright field images (BF).

where **3.AuNP** seems to form the most ordered assemblies. In order to probe the effect that this self-assembly process may have in biological systems we next set about investigating both the cytotoxic and cellular uptake abilities of **1-3.AuNP**.

Cytotoxic studies of 1-3.AuNP *in vitro*

To assess the cytotoxic effects of **1-3.AuNP**, studies were carried out in vitro using the cervical cancer cell line HeLa, and Alamar blue cell viability assay. The cytotoxicity was

reduction in HeLa cell viability when compared to the untreated control cells (Figure 9). Similar results were observed for **1.AuNP** (See ESI). However in the case of **2.AuNP**, a slight reduction in cell viability was observed both in the dark and upon light activation (See ESI).

Fluorescence Confocal Microscopy Studies in HeLa Cells

Fluorescence confocal microscopy was used for real time observation of the complexes within live HeLa cells, the results

of which are shown in Figure 10. The HeLa cells were incubated with the compounds in the dark for various time points and then imaged using fluorescence confocal microscopy. The bright field images (BF), Figure 10, show the morphologies of the treated cells remained similar to the untreated control cells (Figure S21-S22). From the BF images **3.AuNP** can be seen as dense aggregates within the cytoplasm of the cells, which increase or become more dense/darker overtime.

The nucleus of the cells was stained with the nuclear stain DAPI that emits blue fluorescence upon excitation with the 405 nm laser. By exciting the AuNP at the MLCT absorption using a 488 nm laser and measuring the MLCT based emission between 600-700 nm they produce red fluorescence within the live Hela cells (FL channel). In Figure 10 this red fluorescence can be seen to overlap directly with the dense patches observed in the bright field images, confirming the successful uptake of **3.AuNP** into these cells. Despite **1-3.AuNP** not being as luminescent as the free complexes **1-3**, their emission can be clearly seen within the cells. Almost all cells in the field of view contained either the dense patches in the bright field images or red fluorescence due to **3.AuNP**. Moreover, it can be seen that **3.AuNP** was not distributed throughout the cell uniformly, but rather appeared as spots, which over time became brighter and moved closer to the nucleus. By varying the incubation times we concluded that the uptake of the AuNP complexes increased over time and was therefore time-dependent, Figure 10. We also noted that over time the compound moved closer towards the nucleus but there was no evidence of the compounds entering the nucleus of the cells. These results are representative for all compounds (the same results were observed for both **1.AuNP** and **2.AuNP**, Figure S19-S20). We next imaged the HeLa cells that had been treated with **3.AuNP** for 24 h, Figure 11. From these images it was clear that **3.AuNP** was not uniformly distributed throughout the cell but accumulated at one side of the nucleus as seen in the images as black spots or red fluorescence after a period. The emission arising from **3.AuNP** was notably brighter than at the earlier time points as demonstrated in Figure 10, an observation that may suggest either increased fluorescence due to aggregation or an increase in the concentration of **3.AuNP** within the cell over time. These images also confirmed that the **3.AuNP** was not localizing within the nucleus, but instead the results suggest that it may be in vesicle like structures due to the spherical shape of both the 'emission spots' and the dense patches observed in Figure 11b. Hence, these results clearly demonstrate that **3.AuNP** is rapidly taken up by cells and that, whilst the precise localization of the NPs is not clear, accumulation close to the nuclear membrane is observed in HeLa cells by using TEM imaging.

TEM Time Dependent Uptake and Localisation Studies

The time dependent uptake of **3.AuNP** by HeLa cells was also measured using TEM, Figure 12. The results clearly demonstrate that the AuNPs are taken up by HeLa cells over time. Due to the AuNPs favorable size of 15 nm **3.AuNP**,

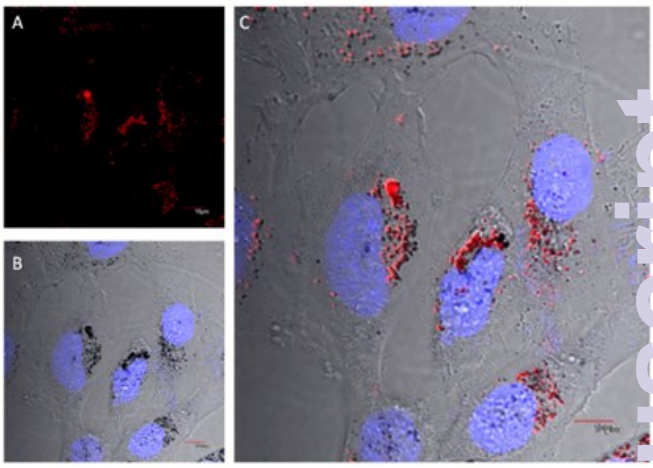

Figure 11. Fluorescence confocal microscopy images of HeLa cells treated wi 20μM **3.AuNP** for 24hr. Fluorescence image (A→C) where nuclear stain DAPI (is blue and **3.AuNP** in red and brightfield images (C).

uptake could be easily imaged and observed as dark sp within the HeLa cells, even after short incubation tim Moreover, Figure 12b, c, e and f, all demonstrated the presence of **3.AuNP** within the HeLa cells in what appear to be endocytic vesicles. The imaging also shows that cells treate with **3.AuNP** have the same morphology as that observed fo the untreated HeLa cells, Figure 12A, confirming that th AuNPs did not exhibit any toxicity towards the cells at tha concentration (20 μM) or exposure time (1-24 hours). The results also confirm our previous observations that **3.AuNP** not toxic towards HeLa cells in the dark. The hig magnification of the TEM images and the larger diameter o **3.AuNP** allowed individual particles to be observed an measured within vesicles, confirming that the AuNPs maintai their original morphology once inside the cells (Figures S2 S25). These results also demonstrate the ease with which suc Ru(II) polypyridyl modified AuNPs can be internalized by cel and suggest that **1-3.AuNP** show significant potential for application in cellular biology as either cargo delivery agent or as diagnostic fluorescence imaging probes. Such factors are further emphasized by the potential to easily functionalize the surfaces of such AuNPs by other Transition met complexes/ligands, etc. The TEM time dependent imaging demonstrated that **3.AuNP** was taken up by the cells within 1-2 hours, and localized within what appear to be single membran vesicles located in the cytoplasm of the cell. Moreover, after 4-6 hours, **3.AuNP** was seen to be located at the nuclear edg (Figure 11) as seen previously in the confocal results in Figure 10. After 24 hours incubation, **3.AuNP** remained in vesicl within the HeLa cell explaining why the AuNPs appeared as spherical aggregates in the brightfield images of our previou confocal images, Figures 10 and 11. There was no evidence from the TEM images of **3.AuNP** free in the cytoplasm or the nucleus of the HeLa cells. These results would confirm th as anticipated the uptake and delivery of **3.AuNP** is by a endocytotic mechanism.

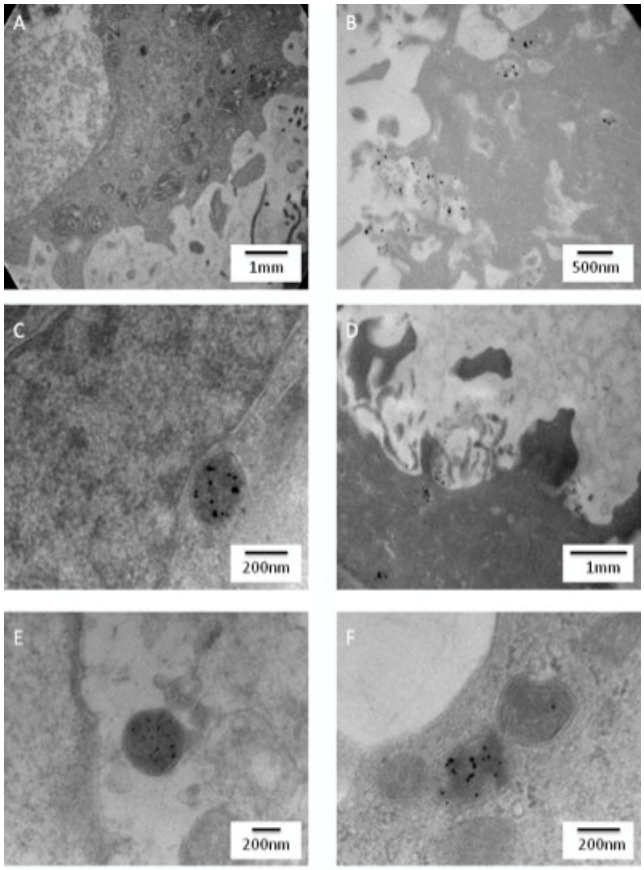

Figure 12. TEM images of HeLa cells incubated with **3.AuNP** (20μM) for (B) 1h (C) 2h (D) 4h (E) 6h (F) 24h or left untreated (A).

We also investigated the uptake and localization of **3.AuNP** in the Murine macrophage cell line; RAW 264.7, using TEM, Figure 13. After 24 h incubation **3.AuNP** was located both inside the RAW cells within vesicle like structures (Fig.13 A-B) and at the outer edge of the cells plasma membrane (Fig.13 C-D). Similar to our studies in HeLa cells individual particles could be visualized within the vesicle but not free in the cytoplasm or in the nuclei of the cells. These results confirm the possibility of endocytosis as the uptake mechanism involved with these large AuNPs. The RAW cells displayed intact membranes and similar morphology to untreated RAW cells (See ESI) further emphasizing **3.AuNPs** lack of dark cytotoxicity.

Conclusion

In this present work we have synthesized three Ru(II) polypyridyl functionalized AuNPs **1-3.AuNP** with an average size of ca. 15 nm, and a hydrodynamic radius of ca. 30 nm. We have demonstrated that these structures are stable in aqueous buffered solution, and that all give rise to absorption spectra consisting of the MLCT absorption contribution from the Ru(II) polypyridyl complexes and from the gold SPR bands. Moreover, upon excitation of the MLCT absorption a red

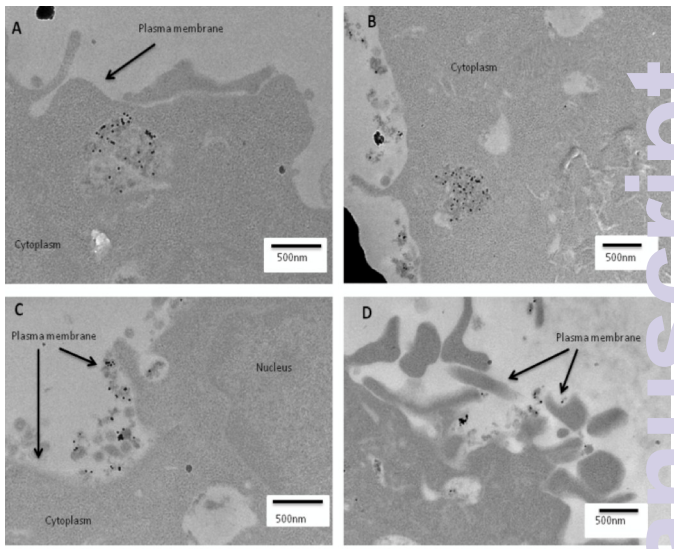

Figure 13. TEM images of RAW 264.7 cells incubated with 20 μM **3.AuNP** for, 24 h**.** Cells were treated then fixed and processed for TEM imaging.

MLCT centered emission is observed, despite quenching by gold surface. We further show, using both TEM and DLS techniques that of the three systems **3.AuNP** is the most highly stable remaining unchanged in solution over a period of 1 hours, even in the presence of buffer, high ionic strength or in the presence of DNA. In the case of **1.AuNP** and **2.AuNP** larger aggregates are formed over time, a phenomenon that becomes more apparent in the presence of DNA. We further demonstrate that these AuNPs are rapidly taken up into live human cancer cells in vitro; the mechanism of which appears to be endocytosis as demonstrated by both TEM and confocal fluorescence microscopic imaging. Upon excitation of the MLCT transition, these AuNPs display red emission within cells with no observed cytotoxicity. We show that these AuNPs are localized within the cytosol, and over time (24 hours) migrate towards the nuclear membrane. Using TEM imaging, we further show that these AuNPs are taken into cells and accumulate within vesicles. Cytotoxic analysis using cell viability assays confirmed that **1-3.AuNP** are relatively non-toxic either in the dark or upon light excitation. Overall, the results from this investigation clearly demonstrate, the potential use of 15 nm Ru(II) functionalized AuNPs as valuable tools for chemical biology. The results obtained from our investigation shed further light on the behavior of **1-3.AuNP** in a biological setting and overwhelmingly support their possible use in cellular applications. We are currently pursuing these and related areas and results will be published in due course.

Experimental

Synthesis of the AuNPs and functionalization with the Ru(II)-polypyridyl complexes: For the preparation of the AuNP we chose the method of reducing gold with sodium citrate, which

resulted in the formation of 15-20 nm AuNP.[23] A solution of $HAuCl_4$ (0.040 g) in Millipore water (300 mL) was boiled at 100 ºC for 15 minutes. To this solution 10 mL of 4.04 x 10^{-2} M sodium citrate solution was added and the solution was left to reflux for another 15 minutes. During this time the solution changed its color from yellow to dark purple to finally turn into a wine color solution, and it was left to cool down to room temperature before using. For the functionalization of the AuNPs with the Ru(II)-polypyridyl complexes a solution was prepared by adding 1 mL of a 0.7 x 10^{-3} M solution of the corresponding Ru(II) polypyridyl complex to 1 mL of the AuNPs solution (3.38 x 10^{-4} M) in water. The mixture was left stirring overnight at pH 3 to improve the loading of the complexes onto the surface of the AuNPs adapting the method of J. Liu et al. in literature.[24] The addition of a concentrated aqueous solution of NH_4PF_6 (0.5 mL) afforded flocculation of a dark solid which was collected by centrifugation and washed with H_2O (3 x 10 mL). The solid was redissolved in MeCN (10 mL) before addition of a conc. solution of TBACl resulted in the formation of a flocculate which was collected by centrifugation and washed with MeCN (3 x 10 mL) before being dried under high vacuum.

Acknowledgments

We thank Science Foundation Ireland (SFI RFP 2009 and SFI PI Awards 10/ IN.1/B2999 and 13/IA/1865), the Ministerio of Economía y Competitividad of Spain (MMC Postdoctoral Fellowship), The Irish Research Council for Science, Engineering and Technology (IRCSET Postgraduate Studentship to RPBE), HEA PRTLI Cycle 4 and TCD for financial support. TEM images were obtained with the help from the CMA facility in TCD and funded by a CMA TEM bursary awarded to Miss Kim Orange in 2013. We like to thank Dr. Sandra Bright for her help and support during this work.

Notes and references

[a] *School of Chemistry and Trinity Biomedical Sciences Institute, Trinity College Dublin, Dublin 2, Ireland. E-mail: gunnlaut@tcd.ie, martinm9@tcd.ie; Tel: +353 1 896 1947, +353 1 896 3459*
[b] *School of Biochemistry and Immunology and Trinity Biomedical Sciences Institute, Trinity College, Dublin 2, Ireland. E-mail: clive.williams@tcd.ie;Tel: +353 1 8962596*
[c] *Department of Chemistry, Maynooth University, National University of Ireland, Maynooth, Ireland.*

† Electronic Supplementary Information (ESI) available: [details of any supplementary information available should be included here]. See DOI: 10.1039/b000000x/

‡ Both authors contributed equally to this work.

1 (a) S. Comby, E. M. Surender, O. Kotova, L. K. Truman, J. M. Molloy and T. Gunnlaugsson, *Inorg. Chem.,* 2014, **53**, 1867 (And references therein). (b) O. R. Miranda, B. Creran and V. M. Rotello, *Curr. Opin. Chem. Biol.,* 2010, **14**, 728. (c) D. J. Lewis and Z. Pikramenou, *Coord. Chem. Rev*., 2014, **273-274**, 213. (d) D. A. Giljohann and C. A. Mirkin, *Nature,* 2009, **462**, 461. (e) E. Boisselier and D. Astruc, *Chem. Soc. Rev.,* 2009, **38**, 1759. (f) S. Eustis, M. A. and El-Sayed, *Chem. Soc. Rev.,* 2006, **35**, 209. (g) J. Park, K. An, Y. Hwang, J.-G. Park, H.-J. Noh, J. Y. Kim, J. Y. Park, J.-H. Hwang and N.-M. Hyeon, *Nat. Mat.,* 2004, **3**, 891. (h) H. Hiramatsu, F. E. Osterloh, *Chem. Mat.,* 2004, **16**, 2509. (i) C. M. Niemeyer, *Angew Chem. Int. Ed.,* 2001, **40**, 4128. (j) Z. Medarova, W. Pham, C. Farre, V. Petkova, A. Moore, *Nat. Med.,* 2007, **13**, 37. (k) J. Massue, S. J. Quinn and T. Gunnlaugsson, *J. Am. Chem. Soc.,* 2008, **130**, 6900. (l) A. J. Hallett, M. Broomfield, P. Christian and S. J. P. Pop, *Transition Met. Chem*., 2014, **39**, 195. (m) A. J. Hallett, P. Christia, J. E. Jones and S. J. A. Pope, *Chem. Commun.,* 2009, 4278.

2 (a) K. Saha, S. S. Agasti, C. Kim, X. N. Li and V. M. Rotello, *Chem Rev.* 2012, **112**, 2739. (b) J. J. Li, D. Hartono, C. N. Ong, B. H. Ba and L. Y. Yung, *Biomaterials,* 2010, **31**, 5996. (c) L. K. Truman, Comby and T. Gunnlaugsson, *Angew. Chem. Int. Ed.*, 2012, **51**, 9624. (d) S. Comby and T. Gunnlaugsson, *ACS Nano*, 2011, **5**, 7184. (e) F. Marano, S. Hussain, F. Rodrigues-Lima, A. Baeza-Squiban and S. Boland, *Arch. Toxicol*., 2011, **85**, 733. (f) B. Kim, G. Han, B. J. Toley, C. K. Kim, V. M. Rotello and N. S. Forbes, *Nature Nanotec* 2010, **5**, 465. (g) J. Drbohlavova, R. Hrdy, V. Adam, R. Kizek, O. Schneeweiss and J. Hubalek, *Sensors*, 2009, **9**, 2352. (h) G. K. Kouassi, J. Irudayaraj, *Anal. Chem*., 2006, **78**, 3234. (i) S. C. Er... L. J. Zu, M. I. Haftel, A. L. Efros, T. A. Kennedy and D. J. Norris, *Nature* 2005, **436**, 91. (j) X. Michalet, F. F. Pinaud, L. A. Bentolila, J. M. Tsay, S. Doose, J. J. Li, G. Sundaresan, A. M. Wu, S. ... Gambhir and S. Weiss, *Science,* 2005, **307**, 538. (k) V. Biju, T. Itoh, A. Anas, A. Sujith and M. Ishikawa, *Anal. Bioanal. Chem*., 200 , **391**, 2469. (l) D. A. Giljohann, D. S. Seferos, W. L. Daniel, M. D. Massich, P. C. Patel and C. A. Mirkin, *Angew. Chem. In. Ed*., 201 , **49**, 3280. (m) N. L. Rosi and C. A. Mirkin, *Chem. Rev.,* 2005, **10** , 1547. (n) K. Huan, P. K. Jain, I. H. El-Sayed and M. A. El-Saye.., *Nanomedicine*, 2007, **2**, 681.

3 (a) D. A. Giljohann, D. S. Seferos, W. L. Daniel, M. D. Massich, P. C. Patel and C. A. Mirkin, *Angew. Chem., Int. Ed.*, 2010, **49**, 3280.(b) S. Rana, A. Bajaj, R. Mout and V. M. Rotello, *Adv. Drug Deliv. Rev.*, 2012, **64**, 200. (c) S. D. Brown, P. Nativo, J. A. Smith, D. Stirling, P. R. Edwards, B. Vengopal, D. J. Flint, J. A. Plumb, D. Graham and N. J. Wheate, *J. Am. Chem. Soc.*, 2010, **132**, 4678. (d) S. Dhar, W. L. Daniel, D. A. Giljohann, C. A. Mirkin and S. J. Lippard, *J. Am. Chem. Soc*., 2009, **131**, 14652. (e) N. Lewinski, V. Colvin, R. Drezek and E. E. Connor, *Small*, 2008, **4**, 26. (f) J. Mwamuka, A. Gole, C. J. Murphy and M. D. Wyatt, *Small*, 2005, **1**, 325. (g) C. M. Goodma , C. D. McCusker, T. Yil-maz and V. M. Rotello, *Bioconjugate Chem.*, 2004, **15**, 897. (h) P. Nativo, I. A. Prior and M. Brust, *ACS Nano*, 2008, **2**, 1639. (i) Y. Cheng, A. C. Samia, J. D. Meyers, I. Panagopoulos, B. Fei and C. J. Burda, *Am. Chem. Soc*., 2008, **130**, 10643. (j) T. A. Taton, C. A. Mirkin and R. L. Letsinger, *Scienc* 2000, **289**, 1757. (k) N. Erathodiyil and J. Y. Ying, *Acc. Chem. Res*., 2011, **44**, 925. (l) C. C. Huang, Z. Yang, K. H. Lee and H. T. Chan , *Angew. Chem., Int. Ed*., 2007, **46**, 6824. (m) P. K. Jain, I. H. El-Sayed and M. A. El-Sayed, *Nano Today*, 2007, **2**, 18. (n) A. ... Prigodich, D. S. Seferos, M. D. Massich, D. A. Giljohann, B. C. Lane and C. A. Mirkin, *ACS Nano*, 2009, **3**, 2147. (o) C. C. You, A. ... Miranda, B. Gider, P. S. Ghosh, I.-B. Kim, B. Erdogan, S. A. Krovi, U. H. F. Buenz and V. M. Rotello, *Nature Nanotec.*, 2007, **2**, 318. (p) M. Liong, J. Lu, M. Kovochich, T. Xia, S. G. Ruehm, A. E. Neil, F. ...

Tamanoi and J. I. Zink, *ACS Nano*, 2008, **2**, 889. (q) M. De, S. Rana, H. Akpinar, O. R. Miranda, R. R. Arvizo, U. H. F. Bunz and V. M. Rotello, *Nature Chem.*, 2009, **1**, 461.

4 (a) N. Hadjiliadis and E. Sletten, *Metal Complex - DNA Interactions*, Wiley-Blackwell, 2009. (b) E. Alessio, *Medicinal Chemistry, Ed. Bioinorganic*, Wiley-VCH Verlag GmbH & Co.: Germany, 2011. (c) K. E. Erkkila, D. T. Odom and J. K. Barton, *Chem. Rev*., 1999, **99**, 2777. (d) R. Zhao, R. Hammitt, R. P. Thummel, Y. Liu, C. Turro and R. M. Snapka, *Dalton Trans*. 2009, **10926**. (e) Q. Yu, Y. Liu, L. Xu, C. Zheng, F. Le, X. Qin, Y. Liu and J. Liu, *Eur. J. Med. Chem*., 2014, **82**, 82. (f) C. A. Puckett and J. K. Barton, *Biochemistry* 2008, **47**, 11711. (g) J. G. Vos and J. M. Kelly, *Dalton Trans*., 2006, 4869. (h) B. Elias and A. K.-D. Mesmaeker, *Coord. Chem. Rev*., 2006, **250**, 1627.(i) A. Ghosh, P. Das, M. R. Gill, P. Kar, M. G. Walker, J. A. Thomas and A. Das, *Chem. Eur. J.*, 2011, **17**, 2089. (j) I. Ortmans, S. Content, N. Boutonnet, A. K.-D. Mesmaeker, W. Bannwarth, J. F. Constant, E. Defrancq and J. Lhomme, *Chem. Eur. J*., 1999, **5**, 2712. (k) G. J. Ryan, S. Quinn and T. Gunnlaugsson, *Inorg. Chem*., 2008, **47**, 401. (l) A. M. Nonat, S. Quinn and T. Gunnlaugsson, *Inorg. Chem*., 2009, **48**, 4646. (m) P. M. Keane, F. E. Poynton, J. P. Hall, I. P. Clark, I. V. Sazanovich, M. Towrie, T. Gunnlaugsson, S. Quinn, C. J. Cardin and J. M. Kelly, *J. Phys. Chem. Lett*., 2015, **6**, 734–738.

5 (a) J. P. Hall, D. Cook, S. Ruiz-Morte, P. McIntyre, K. Buchner, H. Beer, D. J. Cardin, J. A. Brazier, G. Winter, J. M. Kelly and C. J. Cardin, *J. Am. Chem. Soc.*, 2013, **135**, 12652. (b) P. Nordell, P. Lincoln, *J. Am. Chem. Soc*., 2005, **127**, 9670.

6 (a) D. A. Lutterman, A. Chouai, Y. Liu, Y. Sun, C. D. Stewart, K. R. Dunbar and C. Turro, *J. Am. Chem. Soc*., 2008, **130**, 1163. (b) A. Ghosh, P. Das, M. R. Gill, P. Kar, M. G. Walker, J. A. Thomas and A. Das, *Chem. Eur. J.*, 2011, **17**, 2089. (c) I. Ortmans, B. Elias, J. M. Kelly, C. Moucheron and A. K.-D. Mesmaeker, *Dalton Trans*., 2004, **668**. (d) B. Elias, C. Creely, G. W. Doorley, M. M. Feeney, C. Moucheron, A. K.-D. Mesmaeker, J. Dyer, D. C. Grills, M. W. George, P. Matousek, A. W. Parker, M. Towrie and J. M. Kelly, *Chem. Eur. J*., 2008, **14**, 369.

7 (a) S. Neidle and M. Waring, *Molecular Aspects of Anti-cancer Drug DNA Interactions*, Taylor & Francis, Bosa Roca, 1994. (b) I. Kostova, *Curr. Med. Chem*., 2006, **13**, 1085. (c) J.-Q. Wang, P.-Y. Zhang, C. Qian, X.-J. Hou, L.-N. Ji and H. J. Chao, *Biol. Inorg. Chem*., 2014, **19**, 335.

8 (a) M. R. Gill, J. Garcia-Lara, S. J. Foster, C. Smythe, G. Battaglia, J. A. Thomas, *Nature Chem*., 2009, **1**, 662. (b) M. R. Gill, J. A. Thomas, *Chem. Soc. Rev*., 2012, **41**, 3179. (c) S. J. Turrell, M. H. Filby, A. Whitehouse and A. J. Wilson, *Biorg. Med. Chem. Let.*, 2012, **22**, 985.

9 R. B. P. Elmes, J. A. Kitchen, D. C. Williams and T. Gunnlaugsson, *Dalton Trans*., 2012, **41**, 6607.

10 (a) C. Mari, V. Pierroz, S. Ferrari and G. Gasser, *Chem. Sci.*, 2015, **6**, 2660−2686. (b) C. A. Puckett and J. K. Barton, *J. Am. Chem. Soc*., 2009, **131**, 8738.

11 (a) R. B. P. Elmes, K. N. Orange, S. M. Cloonan, D. C. Williams and T. Gunnlaugsson, *J. Am. Chem. Soc*., 2011, **133**, 15862. Other recent examples of Ru(II) based nano-material includes: (b) J. Moreau, F. Lux, M. Four, J. Olesi-ak-Banska, K. Matczyszyn, P. Perriat, C. Frochot, P. Ar-noux, O. Tillement, M. Samoc, G. Ponterini, S. Roux and G. Lemercier, *Phys. Chem. Chem. Phys*., 2014, **16**, 14826. (c) L. He, Y. Huang, H. Zhu, G. Pang, W. Zheng, Y.-S. Wong and T. Chen, *Adv. Mat*., 2014, **24**, 2754. (d) F. C.-M. Leung, A. Y.-Y. Tam, V. K.-M. Au, M.-J. Li and V. W.-W. Yam, *ACS Appl. Mater. Interfaces*, 2014, **6**, 6644. (ef) S. Pramod, P. K. Sudeep, K. G. Thomas and P. V. Kamat, *J. Phys. Chem. B.*, 2006, **110**, 20737. (f) L. Zedler, F. Theil, A. Csáki, W. Fritzsche, S. Rau, M. Schmitt, J. Popp and B. Dietzek, *RSC Adv*., 2012, **2**, 4463. (g) C. R. Mayer, E. Dumas and F. J. Sécheresse, *Colloid Interface Sci*., 2008, **328**, 452. (h) C. R. Mayer, E. Dumas, F. Miomandre, R. Meallet-Renault, F. Warmont, V. Vigneron, R. Pansu, A. Etcheberry and F. Sécheresse, *New J. Chem*., 2006, **30**, 1628. (i) T. Huang and R. W. Murray, *Langmuir*, 2002, **18**, 7077. (j) N. J. Rogers, S. Claire, R. M. Harris, S. Farabi, G. Zikeli, J. B. Styles, N. J. Hodges and Z. Pikramenou, *Chem. Commun*., 2014, **50**, 617. (k) Shani A. M. Osborne and Zoe Pikramenou, *Faraday Discuss*., 2015, DOI: 10.1039/C5FD00108K.

12 (a) E. B. Veale, D. O. Frimannsson, M. Lawler and T. Gunnlaugsson, *Org. Lett.*, 2009, **11**, 4040. (b) E. B. Veale and T. Gunnlaugsson, *J. Org. Chem.,* 2010, **75**, 5513. (c) S. Murphy, S. A. Bright, F. E. Poynton, T. McCabe, J. A. Kitchen, E. B. Veale, D. C. Williams and T. Gunnlaugsson, *Org. Biomol. Chem.,* 2014, **12**, 6610. (d) S. Banerjee, S. A. Bright, J. A. Smith, J. Burgeat, M. Martinez-Calvo, D. C. Williams, J. M. Kelly and T. Gunnlaugsson, *J. Org. Chem*., 2014, **79**, 9272.

13 (a) S. M. Cloonan, R. B. P. Elmes, M. Erby, S. A Bright, F. E. Poynton, D. E. Nolan, S. Quinn, T. Gunnlaugsson and D. C. Williams, *J. Med. Chem.* 2015, **58**, 4494-4505. (b) R. B. P. Elmes, M. Erby, S, M. Cloonan, S. Quinn, D. C. Williams and T. Gunnlaugsson, *Chem. Commun*., 2011, **47**, 686.

14 J. W. Liu and Y. Lu, *Nat. Protoc*., 2006, **1**, 246.

15 (a) T. Huang and R. W. Murray, *Langmuir,* 2002, **18**, 7077; J. Reineck, D. Gómez, H. N. Soon, M. Karg, T. Bell, P. Mulvaney and U. Bach, *ACS Nano*, 2013, **7**, 6636.

16 W. Vanderlinden, M. Blunt, C. C. David, C. Moucheron, A. Kirsch-De Mesmaeker and S. De Feyter, *J. Am. Chem. Soc.*, 2012, **134**, 10214.

17 M. T. Carter, M. Rodriguez and A. J. Bard, *J. Am. Chem. Soc.*, 1989, **111**, 8901

18 R. B. Nair, E. S. Teng, S. L. Kirkland and C. J. Murphy, *Inorg. Chem.*, 1998, **37**, 139.

19 (a) J.-P. Lecomte, A. K.-D. Mesmaeker, M. M. Feeney and J. M. Kelly, *Inorg. Chem*., 1995, **34**, 6481. (b) B. Elias, C. Creely, G. W. Doorley, M. M. Feeney, C. Moucheron, A. Kirsch-Demesmaeker, J. Dyer, D. C. Grills, M. W. George, P. Matousek, A. W. Parker, M. Towrie and J. M. Kelly, *Chem. Eur. J.*, 2007, **14**, 369.

20 (a) A. C. Templeton, J. J. Pietron, R. W. Murray and P. Mulvaney, *J. Phys. Chem. B*., 2000, **104**, 564. (b) C. J. Murphy, A. M. Gole, S. E. Hunyadi, J. W. Stone, P. N. Sisco, A. Alkilany, B. E. Kinard and P. Hankins, *Chem. Commun*., 2008, **544**.

21 M. Eriksson, M. Leijon, C. Hiort, B. Norden and A. Grae-slund, *Biochemistry*, 1994, **33**, 5031.

22 S. Sun, Y. He, Z. Yang, Y. Pang, F. Liu, J. Fan, L. Sund and X. Peng, *Dalton Trans*., 2010, **39**, 4411

23 J. W. Liu and Y. Lu, *Nat. Protoc*., 2006, **1**, 246.

24 X. Zhang, M. R. Servos and J. Liu, *J. Am. Chem. Soc.*, 2012, **134**, 7266.